

# Study of the Stability of the Styrene- and Naphthalene-Choleic Acids by Vapor-Pressure Measurements

Daniela Ferro, Claudio Quaglata, Edoardo Giglio, and Vincenzo Placente\*

*Istituto di Chimica Fisica, Università di Roma, Rome, Italy*

The vaporization behavior of the pure orthorhombic deoxycholic acid and of the styrene- (DCASTY) and naphthalene-choleic acids (DCANAF) was investigated by torsion-effusion method. The vapor pressure of the gaseous guest in equilibrium with its canal complex as a function of temperature was determined: DCASTY,  $\log P$  (kPa) =  $(6.79 \pm 0.20) - (2983 \pm 81)/T$ ; DCANAF,  $\log P$  (kPa) =  $(6.44 \pm 0.22) - (3785 \pm 94)/T$ . The standard enthalpy values of the condensed-phase reaction  $2DCA + X \rightarrow (DCA)_2X$  (where DCA and X represent the deoxycholic acid and the guest molecule, respectively) equal to  $\Delta H^\circ_{298} = 15 \pm 5$  and  $24 \pm 5$  kJ mol<sup>-1</sup> for DCASTY and DCANAF, respectively, were derived. The affinity of the guest molecules for the bile acid in the orthorhombic phase was also considered.

## Introduction

3 $\alpha$ ,12 $\alpha$ -Dihydroxycholeic acid (deoxycholic acid, hereafter referred to as DCA) is a bile acid which forms well-defined molecular compounds, termed choleic acids (1), with a great variety of molecules. As far as we know, DCA (see Figure 1) crystallizes in orthorhombic, hexagonal, and tetragonal phases (2) giving rise to canal complexes with polar and apolar guest molecules. The orthorhombic crystals show the best clathrating ability since they can include many kinds of molecules, especially apolar. Their packing (see Figure 2) is characterized by an assembly of pleated antiparallel bilayers of DCA molecules. A bilayer is stabilized by an efficient scheme of hydrogen bonding (see Figure 3) which presents common features in all of the choleic acids so far studied. The arrangement of the bilayers causes the formation of canals, growing along the *c* axis, with hydrophobic interior surfaces. The size and the shape of the section of the canals can vary within certain limits and depend on the mutual positions along *b* and on the separation along *a* of two adjacent bilayers. Thus, many planar, threadlike and spherical molecules can be accommodated into the cavities.

Generally, the main interactions between host and guest molecules engage the methyl groups protruding from the apolar outer surface of a bilayer. These interactions are particularly strong when the guest molecules are aromatic or possess aromatic groups, as was pointed out in the case of the phenanthrene-choleic acid crystal structure (3).

As a part of a research program, undertaken in order to establish an affinity scale between DCA and guest molecules for the orthorhombic canal complexes, vapor-pressure measurements were performed on DCA alone and the styrene- (DCASTY) and naphthalene-choleic acids (DCANAF). The results obtained for these and other guest molecules can be very useful to foresee which molecules can be preferably occluded in the canal complexes since they are suitable for many applications, for example, the transport of drugs and the polymerization or photochemical reactions.

## Experimental Section and Results

Commercially available DCA (Merck Co.) was purified by crystallizing it from acetonitrile. In order to release the aceto-

nitrile molecules, we heated the crystals at 325 K under reduced pressure ( $\sim 10^{-3}$  kPa) for 10 h. Styrene and naphthalene were pure-grade reagents of commercial origin (Carlo Erba Co.).

DCASTY and DCANAF were prepared by dissolving DCA and styrene in methanol and DCA and naphthalene in ethanol. Colorless prismatic crystals, elongated along *c*, were obtained by slow evaporation.

The DCA obtained as previously described was formed by orthorhombic microcrystals. X-ray powder diagrams showed a close similarity between these diagrams and those of the phenanthrene-choleic acid.

The unit cell dimensions and the space group of DCASTY and DCANAF were determined by oscillation and Weissenberg photographs, using Cu K $\alpha$  radiation. Their densities were measured by means of the Westphal balance, using chloroform and cyclohexane, for DCASTY and by the flotation method, using carbon tetrachloride and cyclohexane, for DCANAF. A Leitz heating plate 350 was employed to measure the melting points at atmospheric pressure.

Some relevant data of DCASTY and DCANAF are reported in Table I.

The vapor pressures of DCA, DCASTY, and DCANAF samples were measured by a torsion-effusion apparatus. The method and the experimental assembly have been described previously (4, 5). The vaporizations were studied by loading with the analyzed sample a particular cell suspended under vacuum on a torsion wire. After the sample was heated, its vapor pressure (*P*) was calculated from the measurements of the torsion angle  $\alpha$  of the wire by the relation  $P = 2K\alpha/(a_1l_1f_1 + a_2l_2f_2)$ , where *K* is the torsion constant ( $0.346 \pm 0.003$  dyn cm rad<sup>-1</sup>) of the used tungsten wire, *a*<sub>1</sub>, *a*<sub>2</sub>, and *l*<sub>1</sub>, *l*<sub>2</sub> are the areas of the effusion orifices and their distances from the rotation axis, respectively, and *f*<sub>1</sub> and *f*<sub>2</sub> are the corresponding geometrical factors derived from the equation (6)  $1/f = 0.0147(R/r)^2 + 0.3490(R/r) + 0.9982$ , where *r* and *R* are the radius and the thickness of the effusion hole, respectively. In Table II are reported the geometrical constants of the used cells.

The temperature of the cell was measured by a calibrated chromel-alumel thermocouple inserted in a cell similar to the torsion one placed below it. Vapor pressures of standard elements (sulfur and lead) were measured by using the different cells and compared with the literature (7) in order to test whether the thermodynamic conditions, the temperature measurements, and the used geometrical factors are reliable.

**DCA.** The packing of the DCA molecules in the bilayers is similar both in the DCA obtained from the releasing of acetonitrile and in DCASTY and DCANAF. Furthermore, only weak van der Waals interactions occur among bilayers, so that the main contribution to the DCA vaporization enthalpy is given by the bilayer disruption.

When the sample was heated, the pressure-temperature curve showed a break at  $472 \pm 5$  K, and the pressure data were not reproducible, probably as a result of an initial decomposition of the sample. At 513 K the vapor pressure fell below the instrument sensibility ( $\sim 10^{-4}$  kPa). At this step of the vaporization, the sample has lost  $\sim 11 \pm 2\%$  of its original weight. When the residue was heated, this presented reproducible vapor-pressure values, and this fact can be taken as

Table I. Some Crystal Data of DCASTY and DCANAF

| <i>a</i> , Å | <i>b</i> , Å | <i>c</i> , Å | <i>Z</i> | <i>d<sub>c</sub></i> , g cm <sup>-3</sup> | <i>d<sub>m</sub></i> , g cm <sup>-3</sup> | space group                                   | host/guest | mp, <sup>a</sup> K   |
|--------------|--------------|--------------|----------|---|---|---|------------|----------------------|
| DCASTY       |              |              |          |   |   |   |            |                      |
| 26.59 ± 0.04 | 13.59 ± 0.02 | 7.28 ± 0.01  | 4        | 1.13 ± 0.02                               | 1.13 ± 0.02                               | P2 <sub>1</sub> 2 <sub>1</sub> 2 <sub>1</sub> | 2:1        | 448 ± 2 <sup>b</sup> |
| DCANAF       |              |              |          |   |   |   |            |                      |
| 26.50 ± 0.04 | 13.72 ± 0.02 | 7.38 ± 0.01  | 4        | 1.13 ± 0.02                               | 1.15 ± 0.02                               | P2 <sub>1</sub> 2 <sub>1</sub> 2 <sub>1</sub> | 2:1        | 457 ± 2              |

<sup>a</sup> The values are measured at atmospheric pressure. <sup>b</sup> At ~436 K it loses styrene.

Table II. Physical Constants of the Used Torsion-Effusion Cells

|   |            | cell A<br>(graphite) | cell B<br>(glass) | cell C<br>(glass) | cell D<br>(graphite) | cell E<br>(graphite) | cell F<br>(graphite) | cell G<br>(graphite) |
|---|------------|----------------------|-------------------|-------------------|----------------------|----------------------|----------------------|----------------------|
| orifice area 10 <sup>-3</sup> (±0.05), <sup>a</sup> cm <sup>2</sup> | semicell 1 | 7.08                 | 6.36              | 9.50              | 0.68                 | 17.67                | 7.85                 | 12.27                |
|   | semicell 2 | 7.08                 | 5.03              | 7.08              | 0.71                 | 17.67                | 7.85                 | 12.27                |
| force correction factors <sup>b</sup>                               | semicell 1 | 0.611                | 0.430             | 0.406             | 0.746                | 0.614                | 0.518                | 0.591                |
|   | semicell 2 | 0.610                | 0.397             | 0.380             | 0.700                | 0.614                | 0.514                | 0.792                |
| moment arm (±0.01), cm  | semicell 1 | 0.81                 | 0.97              | 1.10              | 0.81                 | 0.85                 | 0.89                 | 0.89                 |
|   | semicell 2 | 0.82                 | 1.05              | 0.95              | 0.86                 | 0.84                 | 0.91                 | 0.85                 |

<sup>a</sup> Measured by photographic enlargement. <sup>b</sup> See text.

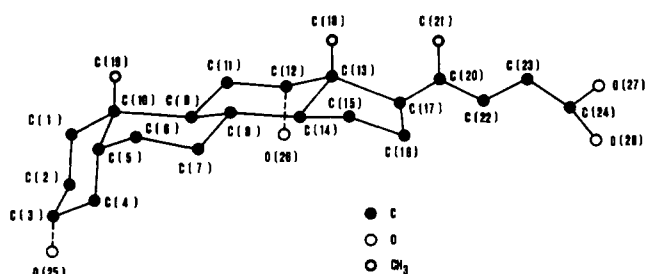


Figure 1. Schematic drawing and atomic numbering of the DCA molecule.

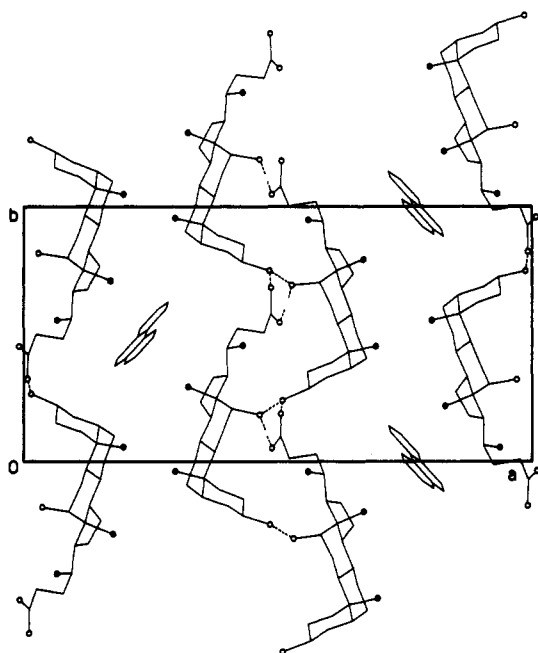


Figure 2. Crystal packing of the phenanthrene-choleic acid viewed along *c*. Black and open circles represent methyl groups and oxygen atoms, respectively. The dashed lines indicate hydrogen bonding.

evidence of its stability. Its molecular weight, equal to  $348 \pm 5$  and deduced from the weight loss, may be explained by the loss of a CO<sub>2</sub> molecule. From the least-squares treatment of the vapor data obtained in each vaporization run, the following average slope and intercept values of the pressure-temperature equation were derived:

$$\log P \text{ (kPa)} = (16.16 \pm 0.24) - (10230 \pm 190)/T$$

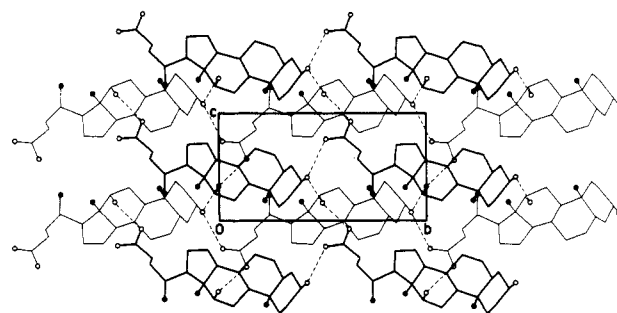


Figure 3. Molecular packing of a bilayer in the phenanthrene-choleic acid viewed along *a*. The symbols have the same meaning as in Figure 2.

Table III. Pressure-Temperature Equation of DCASTY and DCANAF Measured in the First Step of the Vaporization

| sample | expt | cell | temp range, K | no. of points | $\log P \text{ (kPa)} = A - B/T^{\alpha}$ |                |
|--------|------|------|---------------|---------------|---|----------------|
|        |      |      |               |               | <i>A</i>                                  | <i>B</i>       |
| DCASTY | B.01 | D    | 381-412       | 12            | $6.84 \pm 0.28$                           | $2955 \pm 117$ |
|        | B.02 | F    | 353-413       | 16            | $6.90 \pm 0.16$                           | $3017 \pm 61$  |
|        | B.03 | B    | 358-414       | 12            | $6.61 \pm 0.18$                           | $2902 \pm 72$  |
| DCANAF | C.02 | A    | 380-418       | 9             | $6.48 \pm 0.07$                           | $3785 \pm 81$  |
|        | C.03 | G    | 361-419       | 11            | $6.31 \pm 0.38$                           | $3765 \pm 95$  |
|        | C.04 | E    | 385-410       | 10            | $6.55 \pm 0.30$                           | $3811 \pm 136$ |

<sup>a</sup> The associated errors are standard deviations.

where the associated errors were estimated. A panoramic vision of the vaporization behavior of the DCA samples, as measured during four experiments, is graphically reported as  $\log P$  vs.  $1/T$  in Figure 4.

**DCASTY.** The vaporization study of DCASTY was carried out in the temperature range 353-615 K by employing different cells. In the first step of the vaporization was observed a degassing of the samples at ~350 K, probably due to the loss of solvent absorbed or/and occluded for ~1-2% of the sample weight. When the sample was heated further, the vapor-pressure measurements give reproducible values, and their temperature dependence was derived by treating the data by the least-squares method. The corresponding intercept and slope constants are summarized in Table III and plotted in Figure 5. From these values the following pressure-temperature equation was derived:

$$\log P \text{ (kPa)} = (6.79 \pm 0.20) - (2963 \pm 81)/T$$

At  $415 \pm 4$  K the guest activity decreases, and this phenomenon is probably associated with the beginning of a dis-

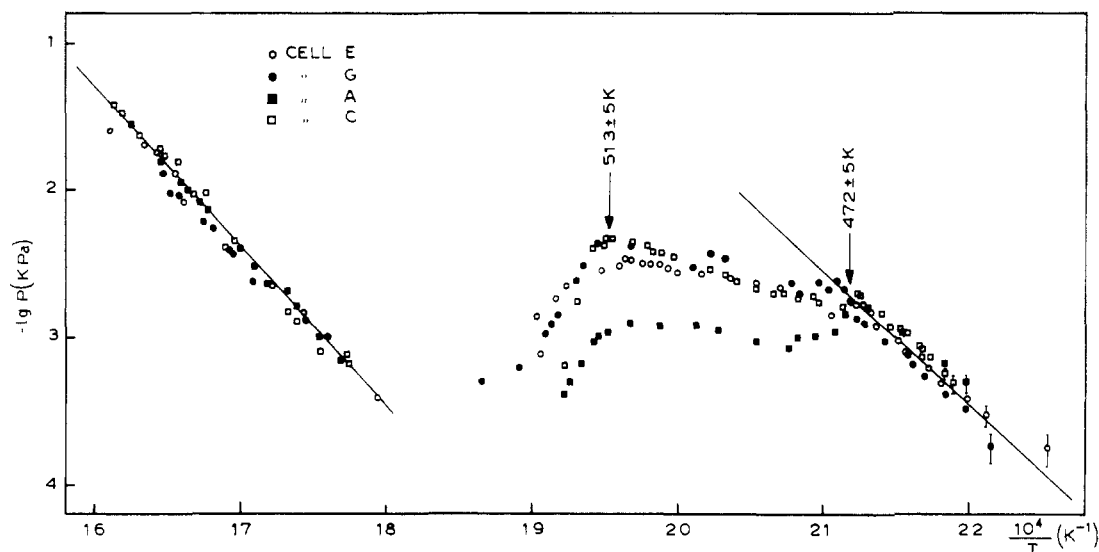


Figure 4. Behavior of the vaporization of DCA.

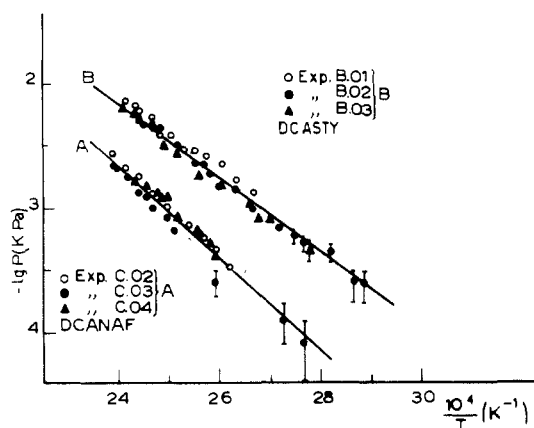


Figure 5. Vapor pressure-temperature dependence of DCASTY and DCANAF in the first step of the vaporization.

ordering in the crystal lattice. After being heated again, the DCASTY showed a rapid increasing of the vapor pressure at both  $430 \pm 5$  and  $450 \pm 5$  K in each experimental vaporization. At the end of this step of the vaporization, all of the guest was practically vaporized from the canal complex and the residue showed a vaporization similar to that found during the study of pure DCA. A panoramic vision of the vaporization behavior of DCASTY (run B.03) is reported in Figure 6.

**DCANAF.** The study of DCANAF vaporization, carried out in the temperature range 361–610 K, showed a behavior similar to that observed in the DCASTY experiments. After an initial degassing the vapor-pressure values over the studied samples were reproducible, and their data are summarized in Table III and plotted in Figure 5. The weight average vapor pressure-temperature equation obtained is

$$\log P (\text{kPa}) = (6.44 \pm 0.22) - (3786 \pm 94)/T$$

At  $425 \pm 3$  K it was noted that the torsion angle decreased. When the sample was warmed further, the DCANAF vapor pressure suddenly increased at both  $435 \pm 4$  and  $452 \pm 4$  K. Also for this compound the residue showed a behavior similar to that observed when vaporizing the pure DCA.

At present we are unable to account for such behavior, similar to that observed for DCASTY. However, it is reasonable to suppose on the basis of the microscopic observation (see also Table I for DCASTY) that the first reported temperature ( $430$  and  $435$  K for DCASTY and DCANAF, respectively) probably corresponds to a rearrangement of the DCA bilayers

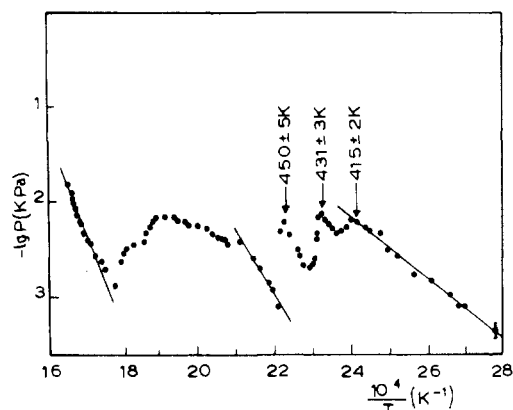


Figure 6. Behavior of the vaporization of DCASTY.

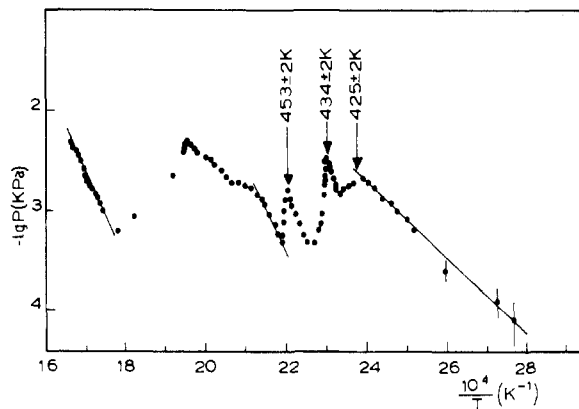


Figure 7. Behavior of the vaporization of DCANAF.

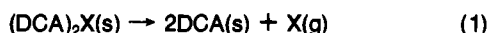
following the almost complete releasing of the guest molecules, whereas the second quoted temperature coincides with that of the sample fusion. Nevertheless, since its interpretation is not essential for the purposes of the present work, we do not attempt to explain it. The vaporization of DCANAF (run C.03) is plotted in Figure 7.

#### Discussion

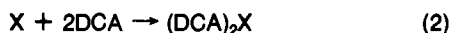
The study of DCA permits one to derive a second-law enthalpy related to its vaporization,  $\Delta H_{460}^{\circ} = 179 \pm 6 \text{ kJ mol}^{-1}$ , and to the vaporization of its stable residue,  $\Delta H_{590}^{\circ} = 209 \pm 4 \text{ kJ mol}^{-1}$ , where the associated errors represent the standard deviations. The experiments carried out with pure DCA showed

that, in the temperature range 350–420 K covered during the first step of the orthorhombic canal complexes investigation, the contribution of the vapor of DCA to the total pressure is negligible and below the instrument sensitivity.

From the pressure–temperature equation determined in this step, the enthalpy change associated with reaction 1 was de-



duced, where X represents the guest. The values  $\Delta H^\circ_{383} = 57 \pm 5$  and  $\Delta H^\circ_{390} = 72 \pm 5$  kJ mol<sup>-1</sup> for DCASTY and DCANAF, respectively, were determined, where the errors were estimated by taking into account only the uncertainties in the temperature measurements. In addition, it is interesting to derive the heat of formation of the canal complexes at 298 K according to the condensed phase reaction (eq 2). Since the mean experi-



mental temperatures are very close to 298 K, the  $\Delta H^\circ_T$  of reaction 1 equal to  $\Delta H^\circ_{298}$  was assumed. Combining these values with the guest vaporization enthalpies  $\Delta H^\circ_{298, \text{vap}} = 42$  (8) and 48 kJ mol<sup>-1</sup> (9) for styrene and naphthalene, respectively, we derived the heats associated with reaction 2:  $\Delta H^\circ_{298} = 15 \pm 5$  and  $24 \pm 5$  kJ mol<sup>-1</sup> for DCASTY and DCANAF, respectively.

The crystal packing of the bilayers formed by DCA molecules is nearly equal in DCASTY and DCANAF, which present only a very small change for the *b* and *c* parameters, connected with the bilayer structure, and for the *a* parameter, influenced by the separation between two adjacent bilayers (2). Moreover, the cell constants of DCASTY and DCANAF are nearly identical with those of the *p*-diiodobenzene–choleic acid, which has the same crystal structure as that found for the phenanthrene–choleic acid (3). Thus, a bilayer packing similar to that of Figure 2 occurs in DCASTY and DCANAF. This statement, supported by van der Waals energy calculations (2), allows us to suppose that the most important host–guest interactions are due to the methyl groups of DCA which point approximately toward the centers of aromatic rings, giving rise to “polarization bonding” involving the  $\pi$  charge cloud, as observed in the phenan-

threne–choleic acid (3). Therefore, it is reasonable to hypothesize that the more polarizable the guest molecule, the more strongly the host–guest interaction occurs. In the case of the aromatic hydrocarbons, for example, it can be expected that the attractive energy between DCA and guest molecules improves by increasing the number of the condensed rings. In this connection the enthalpic values found for DCASTY and DCANAF are in agreement with the above-mentioned trend, styrene being anchored to the methyl groups of DCA more weakly than naphthalene.

Such a study, extended to other guest molecules, can provide useful information for the replacement technique employed in the inclusion polymerization (10). This technique concerns the replacement by new molecules of the guest molecules released from the canals of their corresponding choleic acids by heating. Obviously, the ease of releasing and replacement depends on the size and the shape of the canals as well as on the interaction energy between DCA and guest molecules. Hence, the releasing temperature, which also affects the replacement procedure, may be expressed as an empirical function of the interaction energy. An estimate of this term can be achieved from vapor-pressure measurements and, more roughly, by means of potential-energy calculations.

#### Literature Cited

- (1) Wleland, H.; Sorge, H. Z. *Physiol. Chem.* **1916**, *97*, 1.
- (2) Candeloro De Sanctis, S.; Giglio, E. *Acta Crystallogr., Sect. B* **1979**, *35*, 2650.
- (3) Candeloro De Sanctis, S.; Giglio, E.; Pavel, V.; Quaglata, C. *Acta Crystallogr., Sect. B* **1972**, *28*, 3656.
- (4) Freeman, R. D. In “The Characterization of High Temperature Vapours”; Margrave, J. L., Ed.; Wiley: New York, 1967.
- (5) Placente, V.; De Maria, G. *Ric. Sci.* **1960**, *39*, 545.
- (6) Freeman, R. D.; Searcy, A. W. *J. Chem. Phys.* **1954**, *22*, 762.
- (7) Hultgren, R.; Orr, R. L.; Kelley, K. K. “Select Values of Thermodynamic Properties of Metals and Alloys”; Wiley: New York, 1963.
- (8) Chalyavech, P.; Van Winkle, M. J. *Chem. Eng. Data* **1959**, *4*, 53.
- (9) Fowler, L.; Trump, N. W.; Vogler, C. E. *J. Chem. Eng. Data* **1968**, *13*, 209.
- (10) Miyata, M.; Takemoto, K. *Makromol. Chem.* **1978**, *179*, 1167.

Received for review June 3, 1980. Revised December 9, 1980.

## Densities of Molten KCl–CuCl<sub>2</sub> Obtained by the Automated Float Method

Helge A. Andreassen, Ashok Mahan,<sup>†</sup> and Niels J. Bjerrum\*

The Technical University of Denmark, Chemistry Department A, DK-2800 Lyngby, Denmark

Densities of liquid KCl–CuCl<sub>2</sub> mixtures were measured by using the automated float method. The compositions measured in mole fractions of potassium chloride ( $X_{KCl}$ ) were as follows: 0.4500, 0.5000, 0.6000, 0.6667, and 0.7000. The obtained densities were at each composition fitted to an equation of the form  $\rho = A(X) + B(X)(t - 500)$ .  $A(X)$  and  $B(X)$  were again fitted by polynomials of  $X_{KCl}$  in the mole fraction range 0.4500–1.0000. Finally all of the measured data were fitted to one equation of the form  $\rho = \sum_0^n A_n X^n + (\sum_0^m B_m X^m)(t - 500)$ .

The molten KCl–CuCl<sub>2</sub> system can be used as a catalyst for production of various chlorinated hydrocarbons (1, 2). In connection with a potentiometric investigation of the KCl–CuCl<sub>2</sub> system, density measurements were necessary (3). Because of the dark color of the KCl–CuCl<sub>2</sub> system and the rather high chlorine pressure (0.5 atm at room temperature) necessary to keep the disproportionation of Cu(II) to Cu(I) low, the “automated float method” (4–6) is one of the few methods suited for such a density examination.

#### Experimental Section

The automated float method (4) is based on the use of a differential transformer to detect the passage of quartz floats

<sup>†</sup> Permanent address: Department of Chemistry, University of Allahabad, Allahabad – 211002, India.